

A Self-Replicating Radiation-Shield for Human Deep-Space Exploration: Radiotrophic Fungi can Attenuate Ionizing Radiation aboard the International Space Station

Graham K. Shunk^{1,2*}, Xavier R. Gomez^{1,3}, Nils J. H. Aversch^{4,5*}

¹ Higher Orbits “Go For Launch!” Program

² North Carolina School of Science and Mathematics, Physics Department, Durham NC, United States

³ University of North Carolina at Charlotte, Charlotte, NC, United States

⁴ Department of Civil and Environmental Engineering, Stanford University, Stanford, CA, United States

⁵ Universities Space Research Association, NASA Ames Research Center, Moffett Field, CA, United States

* To whom correspondence should be directed: <graham1118@gmail.com>, <nils.aversch@uq.net.au>

Keywords: Space, Radiation-Shield, Fungus, *Cladosporium sphaerospermum*, Radiotrophic, ISRU

Abstract

The greatest hazard for humans on deep-space exploration missions is radiation. To protect astronauts venturing out beyond Earth’s protective magnetosphere and sustain a permanent presence on Moon and/or Mars, advanced passive radiation protection is highly sought after. Due to the complex nature of space radiation, there is likely no one-size-fits-all solution to this problem, which is further aggravated by up-mass restrictions. In search of innovative radiation-shields, biotechnology holds unique advantages such as suitability for *in-situ* resource utilization (ISRU), self-regeneration, and adaptability. Certain fungi thrive in high-radiation environments on Earth, such as the contamination radius of the Chernobyl Nuclear Power Plant. Analogous to photosynthesis, these organisms appear to perform radiosynthesis, using pigments known as melanin to convert gamma-radiation into chemical energy. It is hypothesized that these organisms can be employed as a radiation shield to protect other lifeforms. Here, growth of *Cladosporium sphaerospermum* and its capability to attenuate ionizing radiation, was studied aboard the International Space Station (ISS) over a time of 30 days, as an analog to habitation on the surface of Mars. At full maturity, radiation beneath a ≈ 1.7 mm thick lawn of the melanized radiotrophic fungus (180° protection radius) was $2.17 \pm 0.35\%$ lower as compared to the negative control. Estimations based on linear attenuation coefficients indicated that a ~ 21 cm thick layer of this fungus could largely negate the annual dose-equivalent of the radiation environment on the surface of Mars, whereas only ~ 9 cm would be required with an equimolar mixture of melanin and Martian regolith. Compatible with ISRU, such composites are promising as a means to increase radiation shielding while reducing overall up-mass, as is compulsory for future Mars-missions.

Introduction

Background

With concrete efforts to return humans to the Moon by 2024 under the Artemis program and establish a permanent foothold on the next rock from Earth by 2028, humankind reaches for Mars as the next big leap in space exploration¹. In preparation for prolonged human exploration missions venturing past Earth-orbit and deeper into space, the required capabilities significantly increase². While advanced transportation solutions led by the private and public sectors alike (BFR/Starship, New Glenn, SLS/Orion) are pivotal and have already reached high technological readiness, life support systems as well as crew health and performance capabilities are equally essential. Therefore, any mission scenario such as ‘Design Reference Architecture 5.0’³ or ‘Mars Base Camp’⁴ (with up to 1000 days of crewed usage), must include innovative solutions that can meet the needs and address the hazards of prolonged habitation on celestial surfaces⁴.

The foremost threat to the short- and long-term health of astronauts on long-duration deep-space missions is radiation⁵. Over one year, the average person on Earth will be exposed to about 6.2 mSv⁶ while the average astronaut on the International Space Station (ISS) is exposed to approximately 144 mSv⁷, and one year into a three-year mission to Mars, an astronaut would already have been exposed to some 400 mSv of radiation, primarily from Galactic Cosmic Radiation (GCR)⁸. While the particular health effects of interplanetary radiation exposure have still not been fully assessed⁹, adequate protection against space-radiation is crucial for missions beyond Earth-orbit, but is more than any other factor restricted by up-mass limitations¹⁰. Both active and passive radiation-shielding, the latter investigating inorganic as well as organic materials, have been and are extensively studied^{11,12}. *In-Situ* Resource Utilization (ISRU) will play an integral role to provide the required capabilities (as well as to break the supply chain from Earth and establish sustainable methods for space exploration because once underway there virtually is no mission-abort scenario)¹³. For ISRU, biotechnology holds some of the most promising approaches, posing useful for providing nutrition¹⁴, producing materials and consumables^{15,16}, and potentially even “growing” radiation shielding¹⁷. Biological studies, however, have so far mostly focused on understanding how organisms protect themselves rather than trying to take advantage of them as biotechnological means for radiation shielding¹⁸.

Nevertheless, there exist many extremophiles that can thrive in highly radioactive environments, namely species of insects, fungi as well as bacteria^{19,20}. Certain fungi can utilize high-energy non-visible radiation through a process termed radiosynthesis²¹, analogous to photosynthetic organisms turning energy from visible light into chemical energy^{22,23}. It is believed that large amounts of melanin in the cell walls of these fungi mediate electron-transfer and thus allow for a net energy gain²⁴. Certain melanized fungi have been found to thrive in highly radioactive environments such as in the cooling pools of the Chernobyl Nuclear Power Plant²³, where radiation levels are three to five orders of magnitude above normal background levels²⁵. Additionally, they have been found to populate the exteriors of spacecraft in low Earth orbit (LEO), where exposure to ionizing radiation is intensified²³.

Here, we explore the opportunity to utilize the dissipation of radiation by melanized fungi as part of a multi-faceted solution to passive radiation-shielding for ISRU^{14,16}. In an additional analysis based on the concept of linear attenuation²⁶, we determine the ability of live melanized fungus as well as the specific contribution of melanin to provide adequate shielding against cosmic radiation.

Concept

This experiment tested the capacity of *Cladosporium sphaerospermum* (a melanized, radiotrophic fungus²¹, cf. supplementary material 1, section A for details) to attenuate ionizing gamma radiation in space. It has been well-documented that *C. sphaerospermum* can survive and even thrive in environments with extreme radiation levels on Earth (e.g. Chernobyl)²⁷. It was hypothesized that similar proliferation occurs in the unique radiation environment of the ISS, which offers the opportunity to test this fungus' response to, and ability to shield from cosmic radiation. The objective was to conduct a proof-of-principle on a single payload, utilizing basic flight hardware for an autonomous experiment which could monitor growth and radiation levels, comparable to an integrated negative-control.

Materials & Methods

Experimental Setup

Space Tango (Space Tango, Inc., Lexington, KY, USA) was contracted for experimental design and construction (terrestrial logistics and on-orbit operations)²⁸. The initial concept for the experimental design was utilized by Space Tango for assembly of the flight-hardware and implementation aboard the ISS within TangoLab™ facilities. The flight-hardware was housed in a 4"×4"×8" double unit standard-size CubeLab™ hardware module (cf. supplementary file 1, figure S1) and consisted of the following main components: two Raspberry Pi 3 Model B+ (Raspberry Pi Foundation, Caldecote, Cambridgeshire, UK) single-board computers, EP-0104 DockerPi PowerBoard (Adafruit Industries, New York, NY, USA), Pocket Geiger Type5, X100-7 SMD (Radiation Watch, Miyagi, JAPAN), Raspberry Pi Camera v2 (Raspberry Pi Foundation, Caldecote, Cambridgeshire, UK) and light source (0.8 W LED-strip) for imaging, DHT22 integrated environmental sensor suite (Aosong Electronics Co. Ltd, Huangpu District, Guangzhou, China) for temperature and humidity readings, a real-time WatchDog™ timer (Brentek International Inc., York, PA, USA), and D6F-P0010A1 (Omron Electronics LLC, Hoffman Estates, IL, USA) electronic flow-measurement system. One Raspberry Pi ("Linux Computer") running Raspbian v10.18 was dedicated to photography, lighting, temperature, humidity, and electronic flow measurement (EFM) readings, while the second Raspberry Pi ("Flight Computer") controlled radiation measurements, stored in a probed Logger Memobox (Fluke Corporation, Everett, WA, USA). The assembled flight-hardware was calibrated and vetted before flight; in particular consistency of the two Geiger counters was confirmed so that no deviation existed between them.

Cladosporium sphaerospermum (ATCC® 11289™) was obtained from Microbiologics (St. Cloud, Minnesota, USA), catalog no. 01254P. Further details on the employed microorganism can be found in supplementary file 1, section A. Growth medium was 39 g/L potato dextrose agar "PDA" from Millipore (Burlington, Massachusetts, USA), catalog no. 110130 (containing 15 g/L agar, 20 g/L glucose, and 4 g/L starch) in a two-compartment split Petri dish (100×15 mm). A total of 20 mL PDA (dyed with orange 1) was used to fill the two compartments of the Petri dish. The plate was sealed with parafilm post-inoculation. With a total height of the Petri dish of 15 mm and a 75 cm² surface area, the thickness of the PDA was ~ 13.33 mm, leaving an approx. 1.67 mm gap for the fungal growth layer. *Cladosporium* hyphae grow to an average of 4 μm in diameter, corresponding to a cellular mass density of approximately 1.1 g/cm³, which was assumed to remain unaffected by microgravity²⁹. The hardware was fully assembled before the inoculation of the agar with *C. sphaerospermum* to minimize the latent growth of the fungus while in transit. A block-chart of the experimental flight hardware setup is given in figure 1 while further details are given in supplementary file 1, section B.

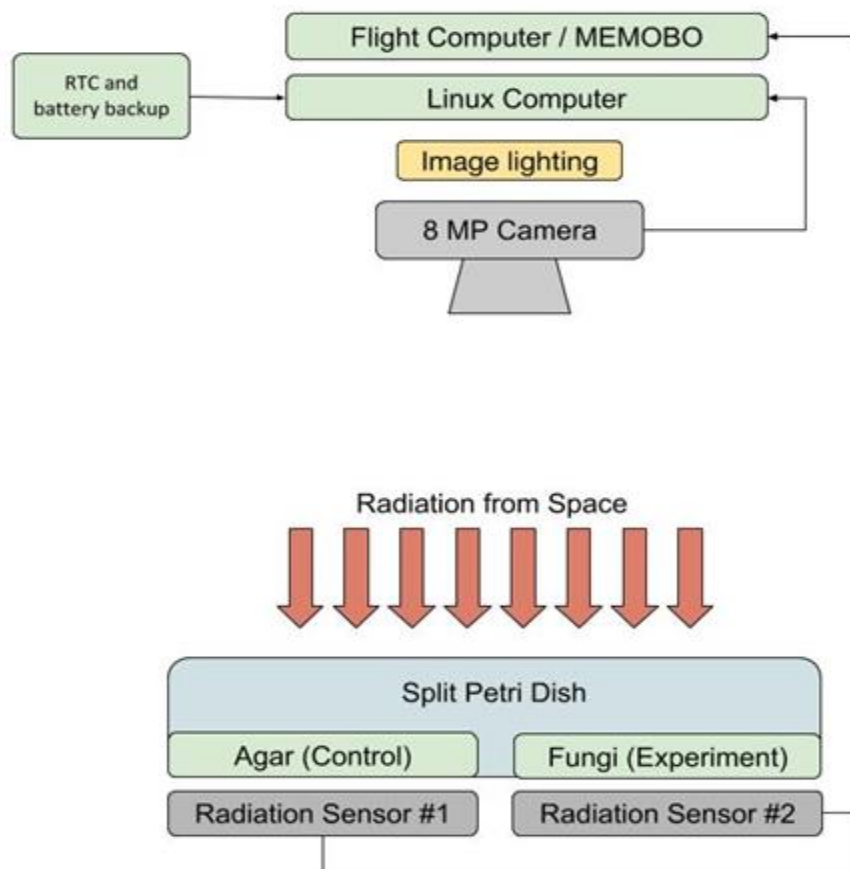


Figure 1: Block-chart of the experimental flight hardware setup. The single (split) Petri dish accommodated both, the experiment (agar + fungus), as well as the control (agar only). The two radiation sensors were situated in parallel directly beneath the Petri dish (one for each side). Note that “shielding” is one-sided only (for simplicity of experimental setup) since radiation is ubiquitous in space. MEMOBO = memory box, MP = megapixel, RTC = real-time clock. Media Courtesy: Space Tango, Inc.

On-Orbit Implementation

The equipment was packaged with the inoculated Petri dish before flight and transported to the ISS in cold storage (4°C) on SpaceX mission CRS-16. The experiment was accommodated in a 2U CubeLab™ (Sealed)³⁰, between Dec 2018 and Jan 2019. Lead-time before the launch was 2 days in cold-stow. Transition time to LEO was 69 hours and 20 minutes (time to “power-on” after inoculation), and the total runtime was 30 days (720 h).

The Petri dish and Geiger counters were oriented so that they faced away from Earth, once on orbit. Pictures of the Petri dish were taken in bursts for the first day of the experimental trial, and every day onward in 30-minute intervals as set by the watchdog timer, while radiation was measured incrementally every ~ 110 seconds. In total 27772 temperature reads for each sensor and 23607 radiation & noise-counts for each Geiger counter were collected. The lab was active aboard the ISS for 30 days with data downlinked on average every 3 days. After 720 h power was cut and the lab awaited return to Earth in June 2019.

Vetting for Cold-Stow

The response of *Cladosporium sphaerospermum* to cold-storage over time was determined in a preliminary experiment. A total of six Petri dishes containing PDA were inoculated with the fungus, five were stored at 4°C with one kept at room temperature (RT) as control. Plates were removed sequentially after 1, 5, 10, 15 and 20 days and incubated at RT. Fungal growth on each plate was monitored and compared to the control.

Evaluation of On-Orbit Growth

Average hexadecimal color values of identical cropped image plots were obtained from photos in intervals of 3 h, and then converted to decimal values. The decimal values were used to generate a growth curve. Further details are given in supplementary file 1, section C.

Evaluation of On-Orbit Radiation

The relative difference in radiation attenuation (in percent) between control and fungus side was determined based on the slope of trendlines fitted to plots of cumulative radiation counts throughout the course of the experiment, as recorded by the Geiger counters of control- and fungus-side. Two stages were defined, the first with no to little fungal growth (0 – 24 h) served as a baseline, while the second with full growth (240 – 720 h) was used to determine the attenuation capacity.

Further, total radiation was quantified in dose equivalents, with an estimate correlation between counts-per-minute (CPM) and radiation dose for the PocketGeiger Type5 of $4 \text{ CPM} \approx 0.075 \pm 0.025 \mu\text{Sv/h}^{31}$, based on the total cumulative recorded counts over the 30 days of the experiment (cf. supplementary file 2).

Radiation Attenuation Analysis

The linear attenuation coefficient (LAC), expressed in cm^{-1} and with the symbol μ , represents the single-beam attenuation capacity of a volume to absorb wavelength radiation at a specified density, while the mass attenuation coefficient (MAC), expressed in cm^2/g and with the symbol μ_m , represents the single-beam attenuation capacity of a volume to absorb wavelength radiation at any density. Attenuation coefficients are dependent on the median surrounding photon energy. Since linear coefficients are dependent on density, mass coefficients are commonly reported, LACs can be derived if the relative density of a given material is known³². The correlations are described by equations 1 – 3, and further assumptions used in the attenuation analysis are given below.

$$\begin{aligned} \text{Eq. 1} & \quad I = I_0 e^{-(\mu/\rho)x} \\ \text{Eq. 2} & \quad \mu_m = \sum w_i \left(\frac{\mu}{\rho}\right)_i \\ \text{Eq. 3} & \quad \mu = (\mu/\rho_m) \times \rho_m \end{aligned}$$

Where Eq. 1 represents the intensity of the beam at distance x and Eq. 2 represents the working linear attenuation coefficient of a material with the mass attenuation coefficient of each material as an input, where w_i is the weight fraction of a material i . Eq. 3 describes the relationship between linear attenuation coefficients, μ , and mass attenuation coefficients, μ/ρ_m .

Only valid for photonic radiation (from 1 keV to 20 MeV)²⁶, calculations based on LACs were based on the assumption that no alpha- and beta- particles could reach the experiment, as neither will be able to penetrate the hull of the ISS³³. Other high-energy (HZE) ions were not respected either, and the analysis focused on ionizing electromagnetic radiation, within the absorption spectrum of the employed Geiger counters (cf. supplementary file 1, section B). Hence, the non-linear influence of secondary radiation, spallation and such could also not be differentiated. Further details are given in supplementary file 1, section D & E.

Results & Discussion

Pre-Flight – Cold-Stow Growth-Test

The ‘Cold-Stow’ experiment showed that for all refrigerated sample-plates there was insignificant fungal growth immediately upon removal from incubation at 4°C (no fungal growth prior to t_0) for all trialed timeframes. Furthermore, all samples exhibited similar growth once at ambient temperature, regardless of the time spent in cold storage.

Flight-Experiment – Growth On-Orbit

Once the hardware was powered on, the temperature rose sharply from the initial of 22°C, reaching 30°C after 4 hours and 31 – 32°C after 8 hours. Past 8 hours, the temperature remained at 31.5±2.4°C for the rest of the experiment (cf. supplementary file 2).

Many dimorphic fungi are characterized by slow growth and need to be incubated for 14 days (at 25°C) for sufficient growth to occur³⁴. However, in the on-orbit lab, *C. sphaerospermum* reached maximum growth after approximately 18 h and full maturity after 48 h, as discernible from figure 2 and the growth curve (figure S2, supplementary file 1). Comparison to the preflight growth tests (supplementary file 1, section C) may indicate that the fungus could experience faster-than-average growth aboard the ISS, due to the utilization of ionizing radiation of the space environment as a metabolic support function, as has been reported for other high-radiation environments: it has previously been shown that *C. sphaerospermum* can experience up to three times faster growth than normal with gamma-rays 500 times as intense as normal^{24,35} [1].

¹ Measured by the dose equivalent, which is 144 mSv/a⁷ for the ISS and 2.4 – 6.2 mSv for Earth⁶, the radiation on the ISS is about 20 – 60 times stronger than the average background on Earth, however 80% of this is attributable to GCR, which is mostly composed of particle radiation. Hence the fraction of (gamma) radiation utilizable by the fungus may not be equivalently significant.

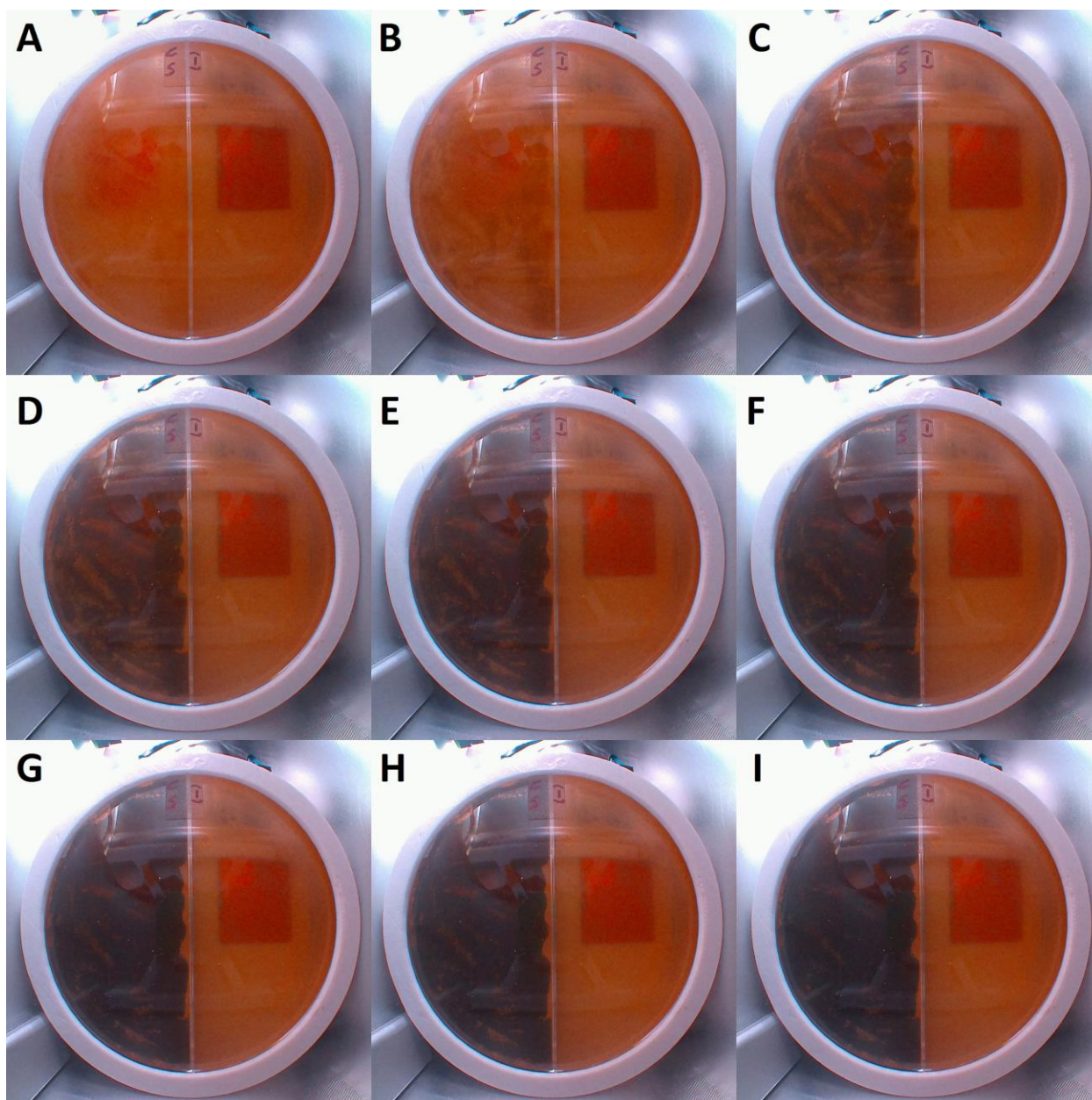


Figure 2 A – I: Photographic data of fungal growth, in intervals of 6 h starting with A: $t_0 = 0$ h continuing until I: $t = 48$ h, shows the development of *C. sphaerospermum* growth by means of optical density on the agar plate in the on-orbit laboratory over the first 48 h of the experiment.

Flight-Experiment – Radiation Attenuation On-Orbit

Observed radiation levels were within expected levels for the ISS, given the specific absorption range of the radiation-sensor (cf. supplementary file 1, section B). Regardless of total measured radiation, most crucial was the accuracy of the relative difference in ionizing events beneath each side of the Petri dish, which had been ensured before flight (data not shown). The radiation levels directly beneath the side of the Petri dish inoculated with *C. sphaerospermum* decreased throughout the experiment (as compared to the control), particularly correlating with microbial growth (figure 3). While there was no significant difference over the first 12 – 24 h, a constant attenuation was observable in the later stage of the experiment. While no further gain in optical density was observed two days into the experiment, the mark of 240 h onward was chosen to determine the attenuation capacity, in order to be conservative. This allowed an additional eight days of maturation before the assumption was made that the fungus did not grow further and melanin content was presumed to be constant and highest. The linearity of the trendlines (figure 3B) supports this conclusion. The full dataset and additional plots of the complete radiation data over the whole course of the experiment can be found in supplementary file 2.

The periodic, slight fluctuations of the radiation, especially recognizable in figure 3A, may be explainable with the orbit time / position of the ISS relative to celestial bodies and orientation of the experiment especially in respect to the sun (either towards or facing away from it). This is supported by the observation that these fluctuations coincide for the recordings of both Geiger counters throughout the entire experiment. For single spikes (as particularly prominent in the incremental plot of radiation events in supplementary file 2), solar events (flare / particle event) are also plausible explanations.

Over the first 24 h of the experimental trial, radiation levels beneath the fungal-growth side of the Petri dish were by average only 0.5% lower. Towards the end of the experiment, an almost 5-fold increase in radiation attenuation could be observed relative to the control side, with average radiation levels 2.42% lower than those of the control (as per the difference of the trendlines' slopes given in figure 3). This showed a direct relationship between the amount of fungal growth (and putatively the melanin content of the biomass) and the amount of ionizing radiation dissipated. With a baseline difference between the two sensors of 0.5% (considering that the fungus may have contributed to this), the observed radiation attenuating capacity can be stated as $2.17 \pm 0.35\%$. Since radiation is ubiquitous in space and only one side of the Geiger counter was shielded by the fungus, it can be postulated that only half of the radiation was blocked. Therefore, it can be extrapolated that the fungus would reduce total radiation levels (of the measured spectrum) by $4.34 \pm 0.7\%$ were it fully surrounding an object. Considering the thin fungal lawn, this shows the ability of *C. sphaerospermum* to significantly shield against space radiation.

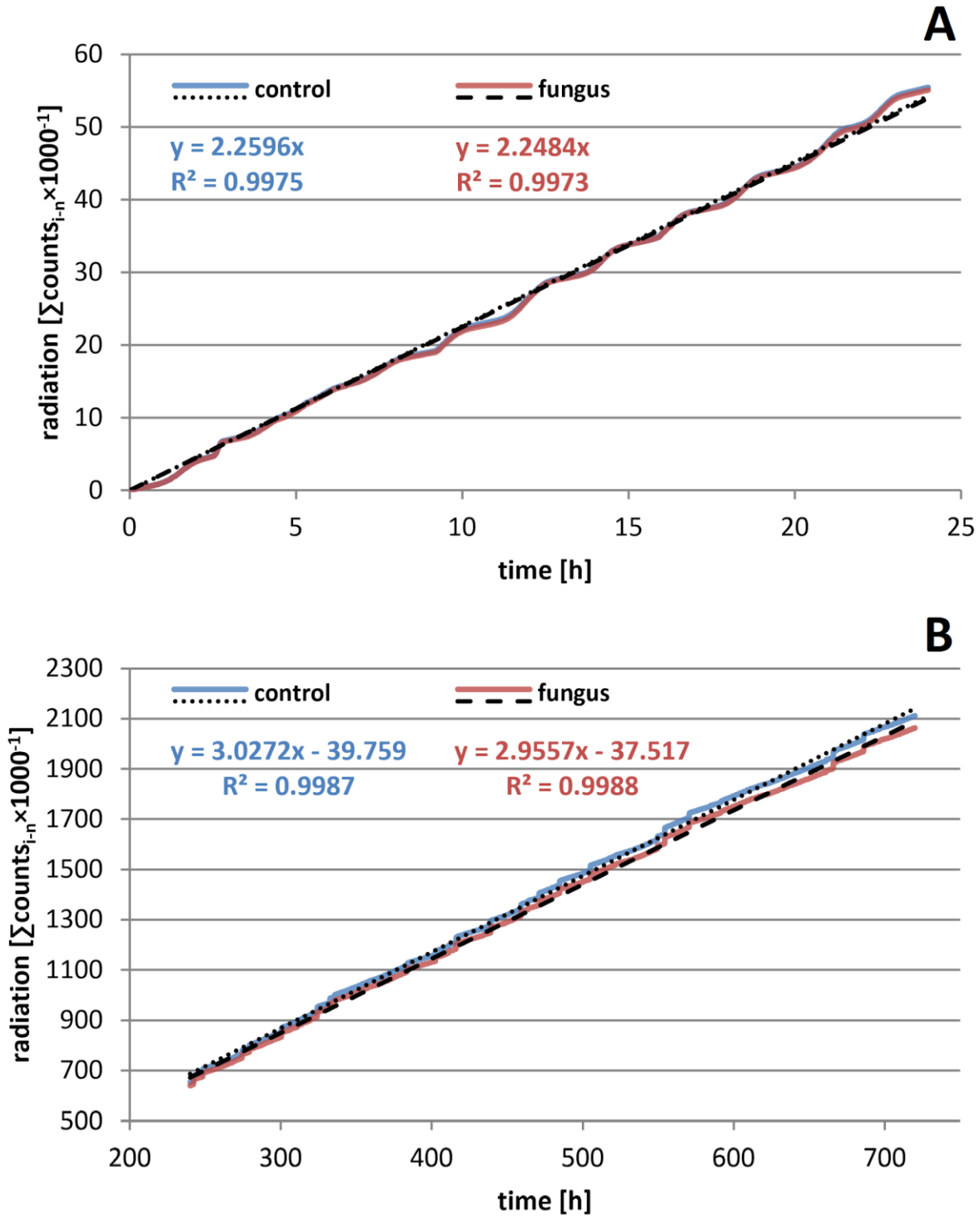


Figure 3 A & B: Cumulative radiation counts of the control and the fungus over time. A: initial phase (0-24 h), B: final $\frac{3}{5}$ of the experiment (240-720 h). For the sake of legitimacy, the cumulative count of ionizing events (radiation) was scaled-down three orders of magnitude ($\times 1000^{-1}$). While in section 'A' the linear trendlines almost coincide, a significant difference in the slope is evident in section 'B' (where the fungus was fully matured), corresponding to an attenuation of the transmitted radiation.

Radiation Attenuation Analysis

The average rates of ionization events over the whole course of the experiment were 48.9 and 47.8 CPM for the control and the fungus side, respectively (cf. supplementary file 2). Based on these numbers, dose equivalents of 0.916 $\mu\text{Sv/h}$ and 0.872 $\mu\text{Sv/h}$ were estimated³¹. This, together with a maximum thickness of $x = 1.67$ mm of the microbial lawn, were the primary figures used in the attenuation analysis. The LAC of *C. sphaerospermum*, μ_{Fungus} , provides a measure for the fungus' capacity to shield against ionizing radiation and allows for further estimations such as the melanin content in the biomass and the required thickness and density of the fungus to provide adequate protection from a certain radiation dose equivalent. Mass and linear attenuation coefficients are presented below while detailed calculations are documented in supplementary file 1, section D.

With Eq. 1, the LAC of *C. sphaerospermum* was determined as $\mu_{\text{Fungus}} = 0.258 \text{ cm}^{-1}$, and with $\rho_m \approx 1.1 \text{ g/cm}^3$ (the average density of fungal biomass)^{29,36}, the MAC for the fungus could be derived as $\mu_{\text{Fungus}}/\rho_m = 0.234 \text{ cm}^2/\text{g}$ according to Eq. 3. At constant photon energies (e.g. 100 MeV), μ_{Fungus} can be compared to other (theoretical) attenuation capacities of common aerospace construction materials and materials considered for passive radiation shielding. Since this experimental LAC is only valid for the specific gamma-energy absorption range of the employed Geiger counters ($\sim 10 \text{ keV}$, cf. supplementary file 1, section B), a corresponding value for space radiation needed to be found. While the theoretical LAC of melanin already allows a comparison with other materials including non-melanized fungal biomass, LACs for melanized fungal biomass can be estimated if the melanin content is known. Here, it was estimated that about 40% by weight of the accumulated *C. sphaerospermum* biomass was composed of melanin (according to Eq. 2, cf. supplementary file 1, section D). This allowed for an estimation of the melanized fungus' LAC at 100 MeV. As can be seen from table 1, its attenuation capacity is significant.

Table 1: Comparison of radiation attenuating capacity of different materials common in spaceflight or proposed for radiation shielding of spacecraft and surface-habitats with melanized/non-melanized fungal biomass and melanin. Attenuation coefficients were generated with the NIST-XCOM mass-attenuation database³², based on molecular formulas and/or densities for the respective materials as referenced, unless trivial or noted otherwise.

Material and literature source for molecular formula and density	Mass Attenuation Coefficient ' μ/ρ ' [cm^2/g] at 100 MeV *	Linear Attenuation Coefficient ' μ ' [cm^{-1}] at relative material density	Reduced dose equivalent [$\mu\text{Sv/h}$] at 6.8 mm material strength [†] outgoing from 30 $\mu\text{Sv/h}$ [§]
Water	0.1707	0.1707	26.71
Non-melanized fungus ^{§ 37}	0.1495	0.1644	26.83
Melanized fungus [#]	0.2508	0.2758	24.87
Melanin	0.2247	0.4044	22.79
Lunar regolith ³⁸	0.2131	0.3197	24.13
Martian regolith ³⁹	0.2653	0.4032	22.81
Aluminosilicate ⁴⁰	0.1554	0.3574	23.53

Aluminum	0.1704	0.4601	21.94
Stainless Steel (301) ⁴¹	0.2553	2.0937	7.225
HDPE	0.1719	0.1667	26.78
BoPET ⁴²	0.1584	0.2186	25.86
Kevlar ⁴³	0.1597	0.2301	25.65
Carbon Fiber Cloth	0.1019	0.1968	26.24
Beta Cloth ⁴⁴	0.0636	0.1399	27.28

[§] based on an empirical elemental formula for the biomass of baker's yeast (*S. cerevisiae*); [#] based on 60% [w/w] non-melanized fungal biomass (baker's yeast)³⁷, and 40% [w/w] melanin content; * chosen based on the photon energy of the inner Van Allen belt of 10 – 100 MeV⁴⁵, and the average photon energy on the surface of Mars of ~ 150 MeV⁴⁶; [†] cumulative hull thickness of the International Space Station (ISS)⁴⁷; [§] based on an estimated average radiation dose of ~ 230 mSv/a on the surface of Mars⁴⁸. HDPE = high-density polyethylene; BoPET = biaxially-oriented polyethylene terephthalate.

Compared among the different materials, water and HDPE (just like other synthetic polymers) have rather small LACs, although they are both highly effective^[2] in shielding against GCR⁴⁶ (foremost high-energy nuclei), as hydrogen-rich compounds are most effective for blocking particle radiation (protons & HZE ions)^{50,51}. This may also serve to explain the low theoretical LAC of non-melanized fungal biomass, which is in a similar range, most likely due to high water content and the low density of biomass^{21,52}. On the other hand, melanin, which makes up a major part of *C. sphaerospermum* biomass (contents of up to 31.5%⁵² and 42.5%⁵³ [w/w] have been reported for melanized fungi), is a very effective attenuator. Using Eq. 2, the melanin-content of the fungus in this experiment was estimated to be around 39 to 44% [w/w] (cf. supplementary file 1, section D for details on assumptions and calculation). This is comparatively high and can be explained with the radiation environment of the ISS, which likely leads to increased melanin production, as reported for other ionizing environments²⁴. Therefore, the predicted high attenuation capacity of a melanized fungus at 100 MeV is a result of the high LAC of melanin. As the remaining biomass has a large water content, the fungus may pose an excellent passive radiation shield for GCR in general (including spallation and Bremsstrahlung⁵⁴, produced due to high proton number).

Often materials with large LACs have high densities and are therefore heavy (like steel and regolith, cf. table 1). However, *C. sphaerospermum*, just like melanin, has a large innate LAC and a low density, making it attractive for aerospace infrastructure. Compared to materials commonly used in space-faring and those being considered for radiation shielding at destinations across the solar system (table 1), it ranks among the best. Beyond having a large LAC, melanin is comparatively lightweight, with a density of approximately 1.6 g/cm³ (in comparison, the density of aluminum is 2.7 g/cm³). Furthermore, while materials such as aluminum or stainless steel largely require manufacturing on Earth and subsequent hauling to celestial bodies, the utilization of melanized fungi may allow for ISRU by means of

² As a material for passive radiation shield against space radiation, polyethylene is currently only being challenged by lithium hydrides⁴⁹.

biotechnology. Due to the saprotrophic nutrition of *C. sphaerospermum*, it grows on virtually any carbon-based biomass, which on Mars could for instance be cyanobacterial lysate, as previously proposed¹⁶.

Regardless of how effective a radiation attenuator may be, passive shielding against GCR is ultimately always limited by mass⁹. For example, to lower the approximate dose equivalent of Martian radiation energy levels to Earth average (from 230 mSv/a to 6.2 mSv/a)^{48,6}, a ~ 21 cm layer of *C. sphaerospermum* would be needed (according to Eq. 1, cf. supplementary file 1, section E for details). Therefore, for a material to have a large MAC, it must be denser. This could be overcome by combining fungal mycelium with other ISRU derived materials, like Lunar or Martian regolith⁵⁵.^[3] An equimolar composite of melanin and Martian regolith would only require a ~ 9 cm thick layer for the same reduction of radiation, as in the example above. The nature of radiotrophic fungi also makes them inevitably/necessarily radioresistant, and thus effectively a self-regenerating and -replicating radiation shield. Through engineered living materials (ELM) technology, integration of synthetic biology with advanced additive manufacturing methods, like 3D bioprinting, may ultimately also allow the creation of smart 'living composite' materials that are adaptive, self-healing and largely autonomous⁶¹.

The density of fungal cultures is limited, however, inevitably also limiting the melanin content of a fungus-regolith composite, but it may become possible to increase the melanin content through metabolic engineering^{56,57} or/and purification of the melanin. This could even allow the manufacturing of attenuators with varying thicknesses, densities, or fractions of other materials. Such composites have already been explored and it has been found that the integration of melanin with other materials can effectively increase the overall attenuation capability of the composite material in a synergistic way (cf. supplementary material 1, section E). The MAC curve of a melanin-bismuth composite, for instance, is more than double that of lead at energies in a low MeV range⁵⁸. Blends or layers of melanin with other materials may yield composites that more efficiently shield against cosmic rays and are effective over the full spectrum of space radiation. This will, however, require extensive further theoretical as well as experimental studies (cf. supplementary file 1, section E).

Conclusion

Through the design of a subtle yet simple experimental setup, implemented as a small single payload, it could be shown that the melanized fungus *C. sphaerospermum* can be cultivated in LEO, while subject to the unique microgravity and radiation environment of the ISS. Growth characteristics further suggested that the fungus not only adapts to but thrives on and shields against space radiation, in accordance with analogous Earth-based studies. It was found that a microbial lawn of only ≈ 1.7 mm already decreased the measured radiation levels by at least 1.82% and potentially up to 5.04%. Attenuation of radiation was consistent over the whole course of the experiment (720 h), allowing a scenario-specific linear attenuation coefficient for *C. sphaerospermum* to be determined. This was further used to approximate the melanin content of the biomass (~ 40%), which corresponds well with literature and served to explain the significant reduction in radiation levels by means of the fungal lawn. Based on the melanin content, the theoretical radiation attenuation capacity of melanized fungal biomass could be put into perspective at constant photon energy levels (100 MeV) with those of materials relevant for future human deep-space exploration missions: melanized biomass as well as pure melanin ranked among the most effective radiation attenuators, emphasizing the great potential they hold as components of radiation shields to protect astronauts from GCR.

³ Regolith has previously been proposed for passive mass-shields in early as well as recent concepts for human exploration of Mars⁵⁷.

Being a living organism, *C. sphaerospermum* self-replicates from microscopic amounts, which opens the door for ISRU through biotechnology, potentially allowing significant savings in up-mass. Often nature has already developed blindly obvious yet surprisingly effective solutions to engineering and design problems faced as humankind evolves – *C. sphaerospermum* and melanin could thus prove to be invaluable in providing adequate protection of explorers on future missions to the Moon, Mars and beyond.

Acknowledgments

As members of ‘Team Orion’ Srikar Kaligotla, Finn Poulin, and Jamison Fuller were instrumental for the conception and planning of the experiment. We cordially extend our thanks to the Higher Orbits Foundation for providing funding for this project through the ‘Go For Launch!’ program, and to Space Tango, for the technical solution, logistics, and implementation of the experiment.

The team would like to specifically express deep gratitude to Michelle Lucas of Higher Orbits, for her guidance and enthusiastic encouragement and to Matthew Clobridge of the Durham County Public Library for bringing the program into reach for the team in the first place, as well as to Gentry Barnett of Space Tango. We would also like to thank Dr. Robert Gotwals for his guidance on the scientific process, and Dr. Jonathan Bennet, who introduced the team to calculations used to interpret the results.

We want to make known our appreciation for our colleagues who supported the research every step of the way and provided encouragement throughout the composition of the manuscript. Finally, we wish to thank our families and friends for their support and encouragement throughout this study.

Author contributions

GKS and XG, in conjunction with colleagues Srikar Kaligotla, Finn Poulin, and Jamison Fuller, conceived of the idea for the study in 2018 and composed the proposal for funding. GKS wrote the initial draft of this paper with support from XG. NJHA joined the team in early 2020, re-visiting and analyzing the data and refined the manuscript. All authors have read and approved the final version of the manuscript. The authors declare no competing interests.

References

1. NASA Artemis. <https://www.nasa.gov/specials/artemis/>. Web 01 Jul. 2020
2. Loff, S. Moon to Mars. NASA <http://www.nasa.gov/topics/moon-to-mars> (2018). Web 01 Jul. 2020
3. Drake, B. G. & Watts, K. D. Human Exploration of Mars Design Reference Architecture 5.0 Addendum #2. 598.
4. Gruenwald, J. Human outposts on Mars: engineering and scientific lessons learned from history. *CEAS Space J.* **6**, 73–77 (2014).
5. Mars, K. Space Radiation Risks. NASA <http://www.nasa.gov/hrp/elements/radiation/risks> (2017). Web 01 Jul. 2020
6. ANS / Public Information / Resources / Radiation Dose Calculator. <https://ans.org/pi/resources/dosechart/msv.php>. Web 01 Jul. 2020
7. Cucinotta, F. A., Kim, M.-H. Y., Willingham, V. & George, K. A. Physical and Biological Organ Dosimetry Analysis for International Space Station Astronauts. *Radiat. Res.* **170**, 127–138 (2008).
8. Letaw, J. R., Silberberg, R. & Tsao, C. H. Galactic Cosmic Radiation Doses to Astronauts Outside the Magnetosphere. in *Terrestrial Space Radiation and Its Biological Effects* (eds. McCormack, P. D., Swenberg, C. E. & Bueker, H.) 663–673 (Springer US, 1988). doi:10.1007/978-1-4613-1567-4_46.
9. Chancellor, J. C. *et al.* Limitations in predicting the space radiation health risk for exploration astronauts. *Npj Microgravity* **4**, 1–11 (2018).
10. Spedding, C. P., Nuttall, W. J. & Lim, S. Energy requirements of a thermally processed ISRU radiation shield for a lunar habitat. *Adv. Space Res.* **65**, 2467–2474 (2020).
11. McCaffrey, J. P., Shen, H., Downton, B. & Mainegra-Hing, E. Radiation attenuation by lead and nonlead materials used in radiation shielding garments. *Med. Phys.* **34**, 530–537 (2007).
12. Ambroglini, F., Battiston, R. & Burger, W. J. Evaluation of Superconducting Magnet Shield Configurations for Long Duration Manned Space Missions. *Front. Oncol.* **6**, (2016).
13. Hall, L. In-Situ Resource Utilization. NASA <http://www.nasa.gov/isru> (2017). Web 01 Jul. 2020
14. Nangle, S. N. *et al.* The case for biotech on Mars. *Nat. Biotechnol.* **38**, 401–407 (2020).
15. Aversch, N. J. H. & Rothschild, L. J. Metabolic engineering of *Bacillus subtilis* for production of *para*-aminobenzoic acid – unexpected importance of carbon source is an advantage for space application. *Microb. Biotechnol.* **12**, 703–714 (2019).
16. Verseux, C. *et al.* Sustainable life support on Mars – the potential roles of cyanobacteria. *Int. J. Astrobiol.* **15**, 65–92 (2016).
17. Nov 1, S. C. / P. & 2019. Biological pigment that acts as nature’s sunscreen set for space journey. *The Hub* <https://hub.jhu.edu/2019/11/01/melanin-space-study/> (2019). Web 01 Jul. 2020
18. Love, STAT, S. What Radiation-Resistant Space Fungus Can Do for Drug Discovery. *Scientific American* <https://www.scientificamerican.com/article/what-radiation-resistant-space-fungus-can-do-for-drug-discovery/>. Web 01 Jul. 2020
19. Kalawate, A. & Mehetre, S. Isolation and characterization of mold fungi and insects infecting sawmill wood, and their inhibition by gamma radiation. *Radiat. Phys. Chem.* **117**, (2015).
20. Krisko, A. & Radman, M. Biology of Extreme Radiation Resistance: The Way of *Deinococcus radiodurans*. *Cold Spring Harb. Perspect. Biol.* **5**, (2013).
21. Eisenman, H. C. & Casadevall, A. Synthesis and assembly of fungal melanin. *Appl. Microbiol. Biotechnol.* **93**, 931–940 (2012).
22. Zhdanova, N. N., Tugay, T., Dighton, J.,

- Zheltonozhsky, V. & Mcdermott, P. Ionizing radiation attracts soil fungi. *Mycol. Res.* **108**, 1089–1096 (2004).
23. Dadachova, E. & Casadevall, A. Ionizing Radiation: how fungi cope, adapt, and exploit with the help of melanin. *Curr. Opin. Microbiol.* **11**, 525–531 (2008).
24. Dadachova, E. *et al.* Ionizing Radiation Changes the Electronic Properties of Melanin and Enhances the Growth of Melanized Fungi. *PLOS ONE* **2**, e457 (2007).
25. Belozerskaya, T. *et al.* Characteristics of Extremophylic Fungi from Chernobyl Nuclear Power Plant. **7** (2010).
26. curtis.suplee@nist.gov. X-Ray Mass Attenuation Coefficients. *NIST* <https://www.nist.gov/pml/x-ray-mass-attenuation-coefficients> (2009). Web 01 Jul. 2020
27. Ledford, H. Hungry fungi chomp on radiation. *Nature news*070521-5 (2007) doi:10.1038/news070521-5.
28. Space Tango, Inc. <https://www.issnationallab.org/implementation-partners/space-tango-inc/>. Web 01 Jul. 2020
29. Bakken, L. R. & Olsen, R. A. Buoyant Densities and Dry-Matter Contents of Microorganisms: Conversion of a Measured Biovolume into Biomass. *Appl. Environ. Microbiol.* **45**, 1188 (1983).
30. Space Tango | TangoLab. *Space Tango* <https://spacetango.com/tangolab/>. Web 01 Jul. 2020
31. Pocket Geiger Radiation Sensor – Type 5 – SEN-14209 – SparkFun Electronics. <https://www.sparkfun.com/products/14209>. Web 01 Jul. 2020
32. curtis.suplee@nist.gov. XCOM: Photon Cross Sections Database. *NIST* <https://www.nist.gov/pml/xcom-photon-cross-sections-database> (2009). Web 01 Jul. 2020
33. NRC: Radiation Basics. <https://www.nrc.gov/about-nrc/radiation/health-effects/radiation-basics.html>. Web 01 Jul. 2020
34. Incubation of fungal cultures: how long is long enough? – Bosshard – 2011 – Mycoses – Wiley Online Library. <https://onlinelibrary.wiley.com/doi/abs/10.1111/j.1439-0507.2010.01977.x>. Web 01 Jul. 2020
35. Castelvechi, D. Dark power: Pigment seems to put radiation to good use. *Sci. News* **171**, 325–325 (2007).
36. Baldwin, W. W. & Kubitschek, H. E. Buoyant density variation during the cell cycle of *Saccharomyces cerevisiae*. *J. Bacteriol.* **158**, 701–704 (1984).
37. Battley, E. H. An empirical method for estimating the entropy of formation and the absolute entropy of dried microbial biomass for use in studies on the thermodynamics of microbial growth. *Thermochim. Acta* **326**, 7–15 (1999).
38. The Chemical Composition of Lunar Soil | Some Meteorite Information | Washington University in St. Louis. <https://sites.wustl.edu/meteoritesite/items/the-chemical-composition-of-lunar-soil/>. Web 01 Jul. 2020
39. Rieder, R. *et al.* The Chemical Composition of Martian Soil and Rocks Returned by the Mobile Alpha Proton X-ray Spectrometer: Preliminary Results from the X-ray Mode. *Science* **278**, 1771–1774 (1997).
40. PubChem. Sodium aluminosilicate. <https://pubchem.ncbi.nlm.nih.gov/compound/19758701>. Web 01 Jul. 2020
41. 301 Stainless Steel Sheet & Coil – AMS 5901. <https://www.upmet.com/products/stainless-steel/301>. Web 01 Jul. 2020
42. e.V, D. G. U. IFA – Databases on hazardous substance (GESTIS): GESTIS database on hazardous substances. <https://www.dguv.de/ifa/gestis/gestis-stoffdatenbank/index-2.jsp>. Web 01 Jul. 2020
43. Cheng, M., Chen, W. & Weerasooriya, T. Mechanical Properties of Kevlar® KM2 Single Fiber. *J. Eng. Mater. Technol.* **127**, 197–203

- (2005).
44. BA 500BC / CF500 F (Beta Cloth, Beta Fabric) – Bron Aerotech.
<https://bronaerotech.com/product/ba-500bc-cf500f-beta-cloth/>. Web 01 Jul. 2020
 45. Friedberg, W. & Copeland, K. Ionizing Radiation in Earth's Atmosphere and in Space Near Earth. 32.
 46. Ehresmann, B. *et al.* Energetic Particle Radiation Environment Observed by RAD on the Surface of Mars During the September 2017 Event. *Geophys. Res. Lett.* **45**, 5305–5311 (2018).
 47. Christiansen, E. L. Design and performance equations for advanced meteoroid and debris shields. *Int. J. Impact Eng.* **14**, 145–156 (1993).
 48. Mars' Surface Radiation Environment Measured with the Mars Science Laboratory's Curiosity Rover | Science.
<https://science.sciencemag.org/content/343/6169/1244797>. Web 01 Jul. 2020
 49. Rojdev, K. & Atwell, W. Investigation of Lithium Metal Hydride Materials for Mitigation of Deep Space Radiation. 11.
 50. Gehrke, N. Utilizing Permanent On-Board Water Storage for Efficient Deep Space Radiation Shielding. *Masters Theses Proj. Rep.* (2018) doi:10.15368/theses.2018.57.
 51. Boulet, P., Collin, A. & Parent, G. Monte Carlo simulation of radiation shielding by water curtains. 11.
 52. Suwannarach, N., Kumla, J., Watanabe, B., Matsui, K. & Lumyong, S. Characterization of melanin and optimal conditions for pigment production by an endophytic fungus, *Spissiomycetes endophytica* SDBR-CMU319. *PLOS ONE* **14**, e0222187 (2019).
 53. Allam, N. G. & El-Zaher, E. H. F. A. Protective role of *Aspergillus fumigatus* melanin against ultraviolet (UV) irradiation and *Bjerkandera adusta* melanin as a candidate vaccine against systemic candidiasis. *Afr. J. Biotechnol.* **11**, 6566–6577 (2012).
 54. Bremsstrahlung | Radiology Reference Article | Radiopaedia.org.
<https://radiopaedia.org/articles/bremsstrahlung>. Web 01 Jul. 2020
 55. Tavares, F. Could Future Homes on the Moon and Mars Be Made of Fungi? NASA
<http://www.nasa.gov/feature/ames/myco-architecture> (2020).
 56. Martínez, L. M., Martinez, A. & Gosset, G. Production of Melanins With Recombinant Microorganisms. *Front. Bioeng. Biotechnol.* **7**, (2019).
 57. Production of Melanin Pigment by Fungi and Its Biotechnological Applications | IntechOpen.
<https://www.intechopen.com/books/melanin/production-of-melanin-pigment-by-fungi-and-its-biotechnological-applications>.
 58. El-Bialy, H. A., El-Gamal, M. S., Elsayed, M. A., Saudi, H. A. & Khalifa, M. A. Microbial melanin physiology under stress conditions and gamma radiation protection studies. *Radiat. Phys. Chem.* **162**, 178–186 (2019).